



## OPEN ACCESS

## EDITED BY

Divita Gupta,  
Universität zu Köln, Germany

## REVIEWED BY

Tarek Trabelsi,  
University of Pennsylvania, United States  
Pablo Pinacho,  
University of Valladolid, Spain

## \*CORRESPONDENCE

Valerio Lattanzi,  
✉ lattanzi@mpg.de

RECEIVED 08 October 2025

REVISED 18 November 2025

ACCEPTED 20 November 2025

PUBLISHED 03 December 2025

## CITATION

Lattanzi V, Sanz-Novo M, Rivilla VM,  
Jiménez-Serra I and Caselli P (2025) Laboratory  
detection and rotational spectroscopy of *trans*-  
HNSO: implications for  
astronomical observations.  
*Front. Chem.* 13:1720662.  
doi: 10.3389/fchem.2025.1720662

## COPYRIGHT

© 2025 Lattanzi, Sanz-Novo, Rivilla, Jiménez-  
Serra and Caselli. This is an open-access article  
distributed under the terms of the [Creative  
Commons Attribution License \(CC BY\)](#). The use,  
distribution or reproduction in other forums is  
permitted, provided the original author(s) and  
the copyright owner(s) are credited and that the  
original publication in this journal is cited, in  
accordance with accepted academic practice.  
No use, distribution or reproduction is permitted  
which does not comply with these terms.

# Laboratory detection and rotational spectroscopy of *trans*-HNSO: implications for astronomical observations

Valerio Lattanzi<sup>1\*</sup>, Miguel Sanz-Novo<sup>2</sup>, Víctor M. Rivilla<sup>2</sup>,  
Izaskun Jiménez-Serra<sup>2</sup> and Paola Caselli<sup>1</sup>

<sup>1</sup>Center for Astrochemical Studies, Max-Planck-Institut für extraterrestrische Physik, Garching bei München, Germany, <sup>2</sup>Centro de Astrobiología (CAB), CSIC-INTA, Madrid, Spain

Sulfur-bearing molecules are central to interstellar chemistry, yet their observed abundances in the gas phase remain far below cosmic expectations in dense interstellar regions. Mixed N–S–O species such as thionylimide (HNSO) are particularly relevant, as they incorporate three key biogenic elements. The *cis* conformer of HNSO has recently been detected in the Galactic Center cloud G+0.693–0.027, but no high-resolution data for the higher energy conformer (*trans*-HNSO) had been available until now. We report the first laboratory detection and rotational spectroscopic characterization of *trans*-HNSO. Spectra were recorded with the Center for Astrochemical Studies Absorption Cell (CASAC) free-space spectrometer employing a hollow-cathode discharge source, yielding 104 assigned transitions between 200 and 530 GHz. A Watson S-reduced Hamiltonian fit reproduced the data with an rms of 40 kHz, providing accurate rotational and centrifugal distortion constants in excellent agreement with CCSD(T) predictions. Although *trans*-HNSO lies only a few kcal/mol above the *cis* form, it has larger dipole components, making its lines particularly intense (more than 5 times brighter, assuming equal abundances) and a very promising candidate for future astronomical detection. The new measurements enable reliable frequency predictions for astronomical searches and will be added to public databases. Combined with recent evidence for tunneling-driven *trans*-to-*cis* isomerization at cryogenic temperatures, these results open the way to test directly whether quantum tunneling governs the interstellar distribution of HNSO isomers.

## KEYWORDS

gas-phase chemistry, rotational spectroscopy, sulfur, interstellar: clouds, interstellar: abundances, astrochemistry

## 1 Introduction

Sulfur chemistry plays a central role in shaping the molecular complexity of the interstellar medium (ISM). Although sulfur is among the ten most abundant elements in the cosmos, with an elemental abundance of  $S/H \approx 1.3 \times 10^{-5}$  relative to hydrogen (Asplund et al., 2009), the observed inventory of sulfur-bearing molecules in the gas phase accounts for only a small fraction of its cosmic value. In dense molecular clouds, where the elemental abundances of other species such as carbon, nitrogen, and oxygen are relatively well reproduced by astrochemical models, sulfur appears to be depleted from the gas phase

by orders of magnitude compared to the cosmic reference abundance. This long-standing discrepancy is known as the “missing sulfur problem” (e.g., Laas and Caselli, 2019).

Several hypotheses have been proposed to explain this missing sulfur reservoir. On the one hand, it may be sequestered in refractory grain mantles in the form of complex polysulfur chains or sulfur polymers such as  $S_8$ , which are difficult to observe spectroscopically (Shingledecker et al., 2020). Recent laboratory simulations have demonstrated that hydrogen sulfide ( $H_2S$ ) can be converted on ice-coated interstellar grains in cold molecular clouds through galactic cosmic-ray processing at 5 K to form sulfanes ( $H_2S_n$ ;  $n = 2-11$ ) and octasulfur ( $S_8$ ) (Herath et al., 2025). This process locks the processed hydrogen sulfide as high-molecular-weight sulfur-containing molecules, providing a plausible rationale for the fate of the missing interstellar sulfur. These sulfur-rich molecules may undergo fractionated sublimation once the molecular cloud transforms into star-forming regions, potentially linking the sulfur chemistry in cold molecular clouds to that in our Solar System.

On the other hand, sulfur could be hidden in unstable or elusive molecular carriers that have not yet been identified due to the lack of laboratory spectra, such as sulfur rings and sulfated polycyclic aromatic hydrocarbon (PASH) molecules (Yang et al., 2024). In this context, the discovery and spectroscopic characterization of new sulfur-bearing molecules are crucial for understanding the distribution of sulfur between gas and dust, constraining chemical models, and enabling targeted astronomical searches with modern observatories.

Beyond this abundance puzzle, sulfur chemistry is deeply intertwined with the chemical evolution of the ISM. Sulfur-bearing molecules participate in both gas-phase and surface reactions, forming diverse functional groups (e.g.,  $-SH$ ,  $-SO$ ,  $-CS$ , and  $-NS$ ) that act as building blocks for more complex species. Many of these compounds—such as  $SO$ ,  $SO_2$ ,  $H_2S$ ,  $OCS$ , and  $HCS^+$ —are also sensitive tracers of energetic and dynamical processes, including shocks, photochemistry, and grain-surface desorption, thereby providing key insights into the physical conditions and evolutionary stages of interstellar environments. The richness and reactivity of sulfur chemistry thus contribute significantly to the molecular diversity observed in space and to the formation pathways of prebiotic molecules. Moreover, sulfur plays a fundamental role beyond the interstellar context. It is a primary product of stellar nucleosynthesis and an important tracer of the chemical evolution of galaxies (Perdigon et al., 2021). In planetary atmospheres, sulfur-bearing species drive complex photochemical cycles that influence cloud formation, temperature regulation, and redox balance (Chang et al., 2023; Gómez Martín et al., 2017; Krasnopolsky, 2012). On Earth, sulfur is deeply integrated into biochemical processes, including enzymatic activity and protein structure through thiol and disulfide linkages (April, 1986). More broadly, sulfur has been recognized as one of the essential ingredients for life, bridging planetary, prebiotic, and biological chemistry (Richardson et al., 2013; Todd, 2022).

Mixed N–S–O species such as thionylimide (HNSO) are particularly attractive targets for laboratory and astronomical studies. These molecules not only contain sulfur, potentially contributing to the missing sulfur reservoir, but also incorporate nitrogen and oxygen, thus standing out as a relevant molecular link

between the interstellar chemistries of these three key prebiotic elements. On Earth, several HNSO isomers have been suggested to connect the biochemistries of nitric oxide (NO) and hydrogen sulfide ( $H_2S$ ), two fundamental gasotransmitters in living beings, further strengthening their astrobiological relevance (Filipovic et al., 2012; Ivanova et al., 2014; Miljkovic et al., 2013; Wu et al., 2018; Zhao et al., 2024). In this context, the laboratory characterization of the rotational spectrum of HNSO is crucial to provide accurate rest frequencies for astronomical searches, particularly in environments rich in sulfur-bearing molecules. Additionally, understanding the stability and relative abundance of its isomers can shed light on the chemical pathways that transform sulfur into different gas-phase and solid-phase carriers, thereby bridging laboratory studies with astronomical observations.

The HNSO system exists as a small family of structural isomers whose relative energies and interconversion barriers critically determine which forms may be present under interstellar conditions. High-level quantum-chemical work has shown that several [N,S,O]-containing isomers (including HNSO and related SNO/NSO species) are close enough in energy that both formation and isomerization are plausible in gas-phase and surface chemistries relevant to the ISM (Kumar and Francisco, 2017). Recent advances in composite quantum-chemical strategies and spectroscopic predictions (which integrate CCSD(T)-quality energetics with anharmonic and core-valence corrections) have further improved the reliability of computed geometries, rotational constants and isomerization barriers for NSO/SNO-type moieties, making such calculations an increasingly powerful complement to laboratory work (Barone et al., 2024). Experimentally, the rotational and rovibrational spectroscopy of thionylimide (HNSO) has a long history, but has been concentrated on the *cis* conformer: the earliest microwave assignment to planar *cis*-HNSO was reported in the late 1960s, and subsequent laboratory studies extended and refined those microwave measurements and the centrifugal-distortion analysis (Dal Borgo et al., 1979; Kirchhoff et al., 1969). Cavity Fourier transform microwave (FT-MW) work later resolved nuclear hyperfine structure in HNSO and its isotopologues, providing precise  $^{14}N$  and D hyperfine parameters (Heineking and Gerry, 1993). High-resolution infrared studies have also characterized several strongly perturbed vibrational bands of HNSO, supplying valuable vibrational-rotational constants and aiding spectroscopic modeling (Puskar et al., 2006).

By contrast, a comprehensive, high-resolution rotational characterization of the *trans* conformer remains absent in the literature. While quantum-chemical calculations indicate that the *trans* form is not more stable than the *cis* conformer, it lies less than 4 kcal/mol higher in energy (Barone et al., 2024; Kumar and Francisco, 2017), suggesting that it could still be appreciably populated under interstellar conditions. Importantly, the *trans* isomer exhibits larger dipole moment components along both the *a* – and *b* – axes compared to the *cis* form, enhancing the intensity of its rotational transitions and making it potentially more detectable in the gas phase despite its slightly higher energy. This is particularly relevant in light of the recent detection of *cis*-HNSO toward the Galactic Center cloud G+0.693–0.027 (G+0.693 hereafter) by Sanz-Novo et al. (2024), where the emission lines were sufficiently intense to derive a significant abundance for the *cis* conformer ( $\sim 4.8$  times lower than  $SO_2$ ).

The detection of high-energy isomers in the ISM has traditionally been viewed with skepticism due to their expected low abundances compared to more stable counterparts (Lattalais et al., 2009). However, recent radioastronomical observations have challenged this view, revealing that several molecular systems contain either entire families of structural isomers or selectively the higher-energy members (e.g.,  $\text{C}_3\text{H}_2\text{O}$ ,  $\text{C}_2\text{H}_4\text{O}_2$ ,  $\text{C}_2\text{H}_2\text{N}_2$ ,  $\text{C}_2\text{H}_5\text{O}_2\text{N}$ , and  $\text{HOCS}^+$ ; Shingledecker et al. (2019); Mininni et al. (2020); Rivilla et al. (2023); San Andrés et al. (2024); Sanz-Novo et al. (2024)). For instance, in the  $\text{HSCO}^+/\text{HOCS}^+$  pair ( $\Delta E = 4.9$  kcal/mol; Wheeler et al. (2006)), only the higher-energy isomer  $\text{HOCS}^+$  has been detected (Sanz-Novo et al., 2024), while within the  $\text{C}_2\text{H}_5\text{O}_2\text{N}$  family, only glycolamide is observed—despite lying 9.7 kcal/mol above the global minimum (N-methylcarbamic acid). These observational results imply that even a higher-energy isomer like *trans*-HNSO, especially with its stronger dipole, could produce detectable emission. The lack of laboratory rotational data suitable for precise astronomical rest-frequency predictions, however, has so far limited targeted searches and incorporation into spectroscopic databases such as CDMS<sup>1</sup> and JPL<sup>2</sup> which hinders its interstellar search, further prompting new dedicated experimental effort.

The present study reports the first laboratory detection and high-resolution rotational spectroscopic characterization of *trans*-HNSO. Using frequency-modulated absorption spectroscopy in the microwave and millimeter-wave regions, we have assigned and analyzed a set of transitions that allow us to determine accurate spectroscopic parameters, including rotational and centrifugal distortion constants. These data provide the foundation for reliable spectral predictions over a wide frequency range, enabling future astronomical searches. In addition, we discuss the astrochemical implications of our findings, particularly regarding the detectability of *trans*-HNSO in sulfur-rich regions of the ISM and its relationship to the *cis* conformer.

## 2 Experimental methods

The measurements were carried out with the Center for Astrochemical Studies Absorption Cell (CASAC), a frequency-modulated free-space absorption spectrometer developed at the Max-Planck Institute for Extraterrestrial Physics (Bizzocchi et al., 2017). CASAC has been used extensively to characterize reactive sulfur-bearing species and other *transient* molecules (e.g., Araki et al., 2024; Inostroza-Pino et al., 2024; Lattanzi et al., 2018; Lattanzi et al., 2024; Prudenzeno et al., 2018), and the present experiments follow the same detection philosophy and instrumental approach.

The primary radiation source was a Keysight E8257D frequency synthesizer phase-locked to a 10 MHz rubidium frequency standard (Stanford Research Systems), providing high absolute frequency accuracy and phase stability. The synthesizer output was amplified and multiplied by Virginia Diodes solid-state active multiplier chains to cover the millimeter and submillimeter bands

(instrumental capability  $\approx 75\text{--}1,600$  GHz). Frequency modulation (FM) was applied at 50 kHz, and the FM signal after interaction with the plasma was detected by a cryogen-free InSb hot-electron bolometer (QMC Instruments Ltd.). The detector output was demodulated with an SR830 lock-in amplifier (Stanford Research Systems) at the second harmonic ( $2f$ ), producing the characteristic second-derivative line shapes of FM absorption spectroscopy. Instrument control, data acquisition and averaging were automated via a computer-controlled acquisition system.

Radiation traversed a 3.0 m long, 5 cm diameter Pyrex absorption tube. For these measurements we employed the hollow-cathode discharge source recently developed in our laboratory and mounted inside the Pyrex tube to create the plasma region used for species production. The hollow-cathode arrangement proved effective at producing and enhancing the concentration of N–S–O reaction products and was used for all reported spectra. A mixture of  $\text{SO}_2$  and  $\text{NH}_3$  gas in a 1:3 ratio diluted in argon was introduced to the cell, yielding a downstream (measured) total pressure of  $\sim 20$  mTorr. The discharge was operated in hollow-cathode mode at 600 V and 85 mA, conditions optimized to maximize the production of the known *cis* isomer while maintaining stable plasma operation. The cell was kept around freezing temperature with a tiny amount of liquid nitrogen to reduce Doppler widths and avoid overheating of the system due to the discharge.

The calibration and initial searches benefited from very strong *cis*-HNSO calibration lines (e.g., Figure 1), which were observed with extremely high intensity and required essentially no extensive exploration of experimental degrees of freedom. These robust *cis* signals were used to verify instrument performance and coarse frequency placement. Upon switching focus to the *trans* conformer, diagnostic scans showed that *trans* lines were detectable after only a few scans; this allowed rapid optimization of the hollow-cathode operating point to the final conditions reported above. Under these optimized settings, individual transitions of the *trans* conformer were observed with good signal-to-noise using minimal averaging, and spectra remained stable over extended acquisitions.

Because many reactive-species experiments can suffer from intrinsically weak absorptions, it is worth noting that the favorable signal strength and stability obtained here substantially simplified line assignment and reduced systematic uncertainty in frequency determination.

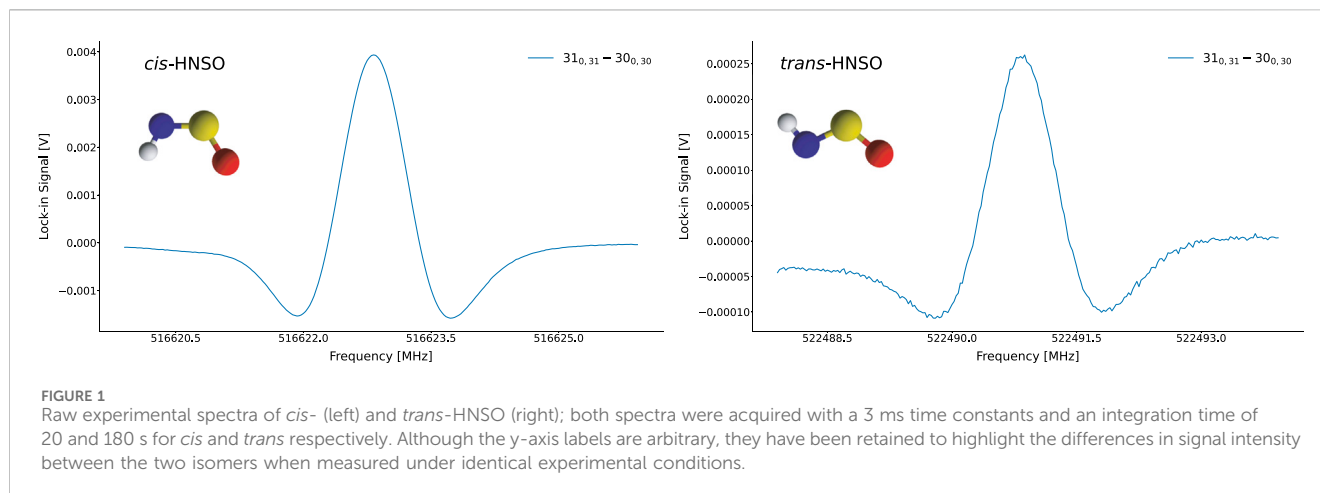
All frequencies reported in this work were measured under the operating conditions given above. Uncertainties reflect combined contributions from line fitting and signal to noise quality; details of the line fitting, Hamiltonian model and uncertainty treatment are given in the Analysis subsection below.

## 3 Theoretical calculations

All quantum-chemical calculations were performed with CFOUR (Coupled-Cluster techniques for Computational Chemistry) (Matthews et al., 2020) using the CCSD(T) model (coupled-cluster with single and double excitations and a perturbative treatment of triple excitations, Raghavachari et al., 1989). Geometries were obtained in the frozen-core approach

1 <https://cdms.astro.uni-koeln.de/>

2 <https://spec.jpl.nasa.gov/>

TABLE 1 Spectroscopic parameters of *trans*-HNSO.

| Parameter      | Unit | Experimental            | Theory (this work) <sup>a</sup> | Theory (previous) <sup>b</sup> |
|----------------|------|-------------------------|---------------------------------|--------------------------------|
| $A_0$          | MHz  | 50429.061 (23)          | 50848.857                       | 50740.9                        |
| $B_0$          | MHz  | 9957.14715 (77)         | 9950.057                        | 9962.9                         |
| $C_0$          | MHz  | 8297.86728 (70)         | 8304.240                        | 8310.3                         |
| $D_J$          | kHz  | 5.6815 (13)             | 5.56824                         |                                |
| $D_{JK}$       | kHz  | -63.432 (54)            | -62.7970                        |                                |
| $D_K$          | MHz  | 1.3911 (31)             | 1.33535                         |                                |
| $d_1$          | kHz  | -1.51879 (24)           | -1.48506                        |                                |
| $d_2$          | kHz  | -0.09954 (23)           | -0.0880475                      |                                |
| $H_J$          | Hz   | 0.00159 (73)            | 0.0072804                       |                                |
| $H_{JK}$       | Hz   | -0.2631562 <sup>c</sup> | -0.2631562                      |                                |
| $H_{KJ}$       | Hz   | -10.9 (14)              | -6.0255433                      |                                |
| # lines        |      | 104                     |                                 |                                |
| $\sigma_{rms}$ | kHz  | 40                      |                                 |                                |
| $\sigma_w^c$   |      | 0.79                    |                                 |                                |

Values in parentheses represent  $1\sigma$  uncertainties, expressed in units of the last quoted digit.

<sup>a</sup>Rotational constants were derived from the equilibrium values obtained at the CCSD(T)/cc-pwCVQZ level and corrected for the vibrational contributions ( $B_e - B_0$ ) estimated at CCSD(T)/cc-pV(T+d)Z. Centrifugal distortion terms derived from anharmonic force field calculations at CCSD(T)/cc-pV(T+d)Z.

<sup>b</sup>From Barone et al. (2024).

<sup>c</sup>Fixed to the theoretical value.

<sup>d</sup>Dimensionless rms, defined as  $\sigma_w = \sqrt{\frac{\sum (\delta_i/err_i)^2}{N}}$ , where the  $\delta$ 's are the residuals weighted by the experimental uncertainty (*err*) and *N* the total number of transitions analyzed.

with cc-pV(X+d)Z (with X = T, Q, 5) Dunning's correlation-consistent polarized valence basis sets of zeta quality with additional tight d-type polarization function added to sulfur (Dunning et al., 2001) to increase the accuracy of the calculated geometries. When considering all electrons in the correlation treatment, the cc-pwCVXZ (X = T and Q) basis sets (Peterson and Dunning, 2002) were used. The best equilibrium structures of *trans*-HNSO have been calculated at the CCSD(T)/cc-pwCVQZ level of theory (Table 1), which has been shown on several occasions to yield equilibrium structures of very high quality for molecules harboring second-row elements (e.g., Lattanzi et al.,

2010). Centrifugal distortion constants were evaluated from anharmonic force-field calculations with second-order vibrational perturbation theory (VPT2) at the CCSD(T)/cc-pV(T+d)Z level.

## 4 Analysis

HNSO exists in *cis* and *trans* conformers with *cis* being 3.7 kcal/mol (~1860 K) relatively more stable (see Supplementary Figure S1), and a *cis-trans* conversion barrier of 14.5 kcal/mol (at the CCSD(T)/aug-cc-pV5Z//CCSD(T)/aug-cc-pVTZ level; Kumar and Francisco

2017). The *trans*-HNSO is an asymmetric-top rotor very close to the prolate limit ( $\kappa = -0.92$ ) with a  $C_s$  symmetry and a quasi planar structure (inertial defect of  $\Delta \approx 0.128 \text{ amu } \text{\AA}^2$ ). The present rotational analysis is based on a dataset of 104 distinct microwave transitions fitted with 11 spectroscopic parameters (see Table 1), covering the frequency interval  $\sim 200\text{--}530 \text{ GHz}$  and sampling upper-state quantum numbers up to  $J = 31$  and  $K_a$  up to 6. This combination of line density,  $J$ -range and  $K_a$ -coverage gives good leverage on all three principal rotational constants and on the leading centrifugal-distortion terms required to model the measured molecule. To determine the central frequencies of the observed transitions, each averaged experimental spectrum was first baseline-corrected and then fitted using a modulated Voigt line-shape function (Dore, 2003). The fitting procedure was carried out with QtFit, a routine included in our in-house Python library for laboratory spectroscopy (pyLabSpec<sup>3</sup>). In order to reproduce subtle line-shape effects, the analysis also accounted for both the dispersive component of the Fourier transform of the dipole correlation function and a low-order polynomial term (typically second or third order). These additional contributions compensate for line asymmetry and residual baseline structure caused by standing waves within the absorption cell due to imperfect transmission of the window materials.

Fitting the observed transitions with a Watson S-reduced Hamiltonian yielded an overall standard deviation of 40 kHz (see Table 1). Individual transitions uncertainties were set to 50 kHz for the majority of lines, while three particularly weak transitions were assigned larger uncertainties of 100 kHz. The normalized rms (reduced  $\chi^2$  equivalent) is 0.79, i.e., very close to unity, which implies that the adopted experimental uncertainties and the Hamiltonian model are mutually consistent and that no overall inflation of the uncertainties is required.

The quantum-number coverage makes the dataset sensitive to the three principal rotational constants ( $A, B, C$ ) and to both diagonal and off-diagonal centrifugal distortions. In addition, earlier theory predicts appreciable  $\mu_a$  – and  $\mu_b$  – dipole moment components for the *trans* conformer (1.96 D and 2.41 D derived from our calculations at CCSD(T)/cc-pwCVQZ level). No obvious systematic residual structure attributable to partially resolved nuclear hyperfine splitting is apparent at the present resolution, linewidth, and RMS level, considering also the quantum number coverage of the present dataset ( $J_{\min} = 10$ ) and the collapse of the hyperfine structure with higher  $J$ 's. The hyperfine structure from  $^{14}\text{N}$  might be discoverable by a dedicated search in the radio band in our molecular jet expansion system coupled with our chirped-pulse spectrometer (CASJet+CP-FT).

The rotational constants are determined experimentally with very high precision (uncertainties from a few  $10^{-2} \text{ MHz}$  down to  $10^{-5} \text{ MHz}$ ). The theoretical values at the quoted level (CCSD(T)/cc-pwCVQZ and corrected for the vibrational contribution estimated at CCSD(T)/cc-pV (T+d)Z), are in good agreement, especially for  $B$  and  $C$  with differences that are small in absolute terms ( $B$ : 17 MHz,  $C$ : 7 MHz), and correspond to fractional deviations of  $\leq 0.07\%$ . These small differences are consistent with expectations for the level

of the quantum chemical calculated geometries that do not include full vibrational averaging and complete-basis extrapolation. The excellent match confirms the conformational assignment and indicates that the calculated geometry captures the heavy-atom framework with high fidelity. Overall also the quartic distortion constants agree to within a few percent—a level of correspondence that is satisfactory given that centrifugal constants are particularly sensitive to the chosen level of theory (harmonic force field vs. full anharmonic treatment) and to vibrational corrections. The relatively larger fractional discrepancy seen for the smallest parameters (e.g.,  $d_2$ ) is expected because when the absolute magnitude is tiny even small absolute differences produce large relative percentages; in practice the absolute differences here are only a few  $10^{-3} - 10^{-2} \text{ kHz}$ .

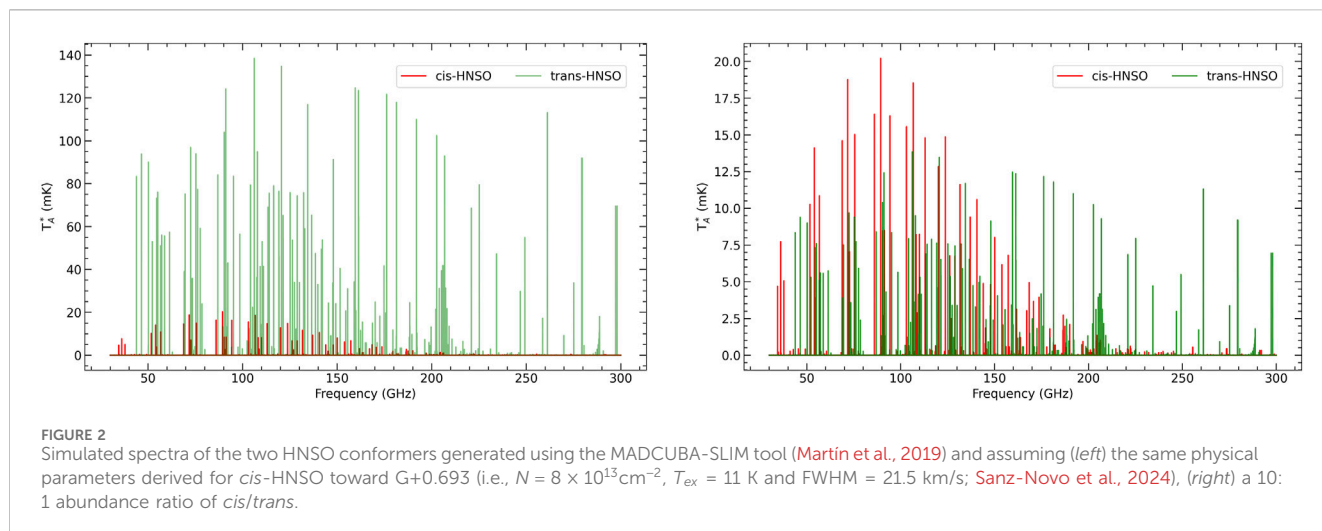
Only three sextic parameters were used in the model to reproduce the experimental lines within the estimated uncertainties. One of these, namely,  $H_{JK}$ , was kept fixed to the *ab initio* calculated value since the frequency/quantum number coverage was not able to efficiently constrain it, although removing it completely worsened the overall fit. The remaining sextic parameters were marginally determined from the data and, although their formal uncertainties are larger than those of the rotational and quartic distortion constants, their absolute magnitudes are small and their inclusion materially improves the reproduction of the high-frequency lines within the measured range. In particular, the experimental values for  $H_J$  and  $H_{KJ}$  provide useful empirical anchors that, together with the calculated values, enable confident predictions of transition frequencies across the observed band.

## 5 Discussion and conclusion

The present study reports the first high-resolution rotational characterization of *trans*-HNSO, establishing a robust spectroscopic foundation for its astronomical detection and placing the molecule in a broader astrochemical context. The results provide both accurate rest frequencies and a deeper understanding of how this conformer compares with theoretical expectations, while also highlighting the implications of its potential presence in space. Our dataset yields rotational and centrifugal distortion constants of remarkable precision, with an overall rms deviation of 40 kHz, and a general good agreement with the couple-cluster predicted values. By combining experimentally determined constants with selected theoretical values where necessary, we obtain a balanced set of parameters that provides highly reliable frequency predictions within the measured region, while maintaining controlled extrapolation beyond it.

Two features make *trans*-HNSO a promising target for radioastronomical searches. First, its dipole moment has substantial components along both the  $a$ - and  $b$ -axes, ensuring that a wide range of transitions exhibit significant intensities. Second, the present frequency determinations are anchored with sub-50 kHz accuracy, far surpassing the resolution requirements imposed by typical interstellar line widths, such as the case of G+0.693 with typical linewidths of about 15–20 km/s ( $\sim 5\text{--}7 \text{ MHz}$  at 100 GHz; Requena-Torres et al., 2008; Zeng et al., 2018). These qualities suggest that, provided it reaches detectable abundances, *trans*-HNSO can be securely identified in observational

3 <https://laasworld.de/pylabspec.php>



spectra (see Figure 2). With an estimated frequency accuracy on the order of a few tens of kHz for the strongest transitions in the Q band (33–50 GHz) and the 3 mm band (~80–120 GHz), the spectroscopic database derived from our new measurements provides a reliable basis for the identification of this conformer also in cold Galactic environments, such as TMC-1, where molecular emission lines typically exhibit linewidths of 0.5 km/s (167 kHz).

This motivation is strengthened by the recent detection of the *cis* isomer in the Galactic Center cloud G+0.693 (Sanz-Novo et al., 2024), where its lines were strong enough to permit abundance estimates. Moreover, G+0.693 has already emerged as a uniquely rich source of molecular stereochemistry, with several distinct stereoisomers detected toward this cloud (e.g., the *Z*- and *E*-conformers of cyanomethanimine (Rivilla et al., 2019), *cis* and *trans* HCOOH (Sanz-Novo et al., 2023), *n*-propanol *n*-C<sub>3</sub>H<sub>7</sub>OH (*n*-C<sub>3</sub>H<sub>7</sub>OH; Jiménez-Serra et al., 2022), the high-energy *trans* conformer of carbonic acid, HOCOOH (Sanz-Novo et al., 2023), *trans* methyl formate (Sanz-Novo et al., 2024) and *cis* N-methylformamide (Zeng et al., 2025). The coexistence of multiple isomeric forms in the same environment indicates that both formation and survival of higher-energy isomers are feasible under specific interstellar conditions. Given that the *trans* conformer is only a few kcal/mol less stable than *cis*-HNSO, but possesses larger dipole moments, it may therefore be present with the current levels of sensitivity of the above ultra-deep survey. Sources such as G+0.693, Sgr B2(N), Orion KL, and shocked outflows thus represent natural starting points for targeted searches. To support such efforts, the spectroscopic parameters derived here will be incorporated into public databases, such as CDMS.

The simultaneous availability of *cis* and *trans* spectroscopic data opens new avenues for using their relative abundances as probes of interstellar chemistry. A dominance of *cis*-HNSO would point to low-temperature formation pathways or grain-surface synthesis with limited energy available for isomerization. By contrast, the detection of *trans*-HNSO at appreciable levels would indicate either gas-phase routes capable of producing the higher-energy conformer or in general other competitive chemical processes that promote isomerization in the gas phase (as e.g., multidimensional small curvature tunneling effects; García de la Concepción et al., 2022).

Quantifying the *cis/trans* ratio in different environments would therefore provide direct constraints on the dominant chemical routes of sulfur–nitrogen–oxygen chemistry in the ISM (see also Molpeceres et al., 2025).

Since extrapolation toward lower frequencies is generally reliable when higher-frequency measurements are available, predictions up to the measured range should be regarded as sufficiently accurate for radioastronomical identification. However, further improvements might be desirable to refine the quality of extrapolations when higher frequency transitions are needed. Extending the measurements to higher frequencies and higher *J* levels would provide tighter constraints on sextic and higher-order distortion parameters. Complementary isotopologue studies could deliver independent structural constraints and reduce correlations among centrifugal constants. In this context, the relatively high abundance observed for *cis*-HNSO makes its <sup>34</sup>S isotopologue a particularly promising target, motivating new dedicated laboratory measurements. Moreover, low frequency, i.e., radio/microwave spectroscopy could probe the lowest-frequency transitions with sub-kHz precision, potentially resolving hyperfine structure and thereby enhancing catalog accuracy. Parallel theoretical work, including vibrational corrections and higher-level treatments of electron correlation, will also help to benchmark the most delicate parameters.

An intriguing additional dimension to the problem of HNSO isomerism has recently been provided by Jiang et al. (2025), who demonstrated that *trans*-HNSO generated photochemically in cryogenic matrices undergoes rapid conversion back to the *cis* form via quantum tunneling, with a half-life of only minutes at 3 K. While these results clearly indicate efficient tunneling-driven isomerization under matrix-isolation conditions, it remains uncertain to what extent such behavior would persist in the gas phase or in astrophysical environments. The precise spectroscopic constants reported here now enable this hypothesis to be tested observationally. If *trans*-HNSO is detected in regions where *cis*-HNSO is abundant, it would indicate that tunneling is less effective under interstellar conditions than in laboratory ices, perhaps due to environmental differences or competing processes, and in the gas phase, as suggested by García de la Concepción et al. (2021) to

explain the E/Z isomer ratio of several imines detected in the ISM. Conversely, if *trans*-HNSO remains systematically undetected despite favorable conditions, it would strongly support the view that tunneling controls its astrochemical fate. In either outcome, astronomical observations made possible by this work will provide an unprecedented opportunity to connect molecular quantum dynamics at cryogenic temperatures with the chemical inventories observed in space.

## Data availability statement

The raw data supporting the conclusions of this article will be made available by the authors, without undue reservation.

## Author contributions

VL: Validation, Conceptualization, Data curation, Visualization, Project administration, Formal Analysis, Software, Writing – review and editing, Methodology, Investigation, Supervision, Writing – original draft. MS-N: Supervision, Software, Methodology, Data curation, Writing – original draft, Conceptualization, Writing – review and editing, Investigation, Visualization. VR: Supervision, Writing – review and editing, Funding acquisition, Resources, Project administration, Validation. IJ-S: Resources, Validation, Project administration, Writing – review and editing, Funding acquisition, Supervision. PC: Resources, Writing – review and editing, Funding acquisition, Validation, Project administration, Supervision.

## Funding

The authors declare that financial support was received for the research and/or publication of this article. We gratefully acknowledge the Max Planck Society for the financial support. VR, MS-N, and IJ-S acknowledge funding from the grant no. PID2022-136814NB-I00 by the Spanish Ministry of Science, Innovation and Universities/State Agency of Research MICIU/AEI/10.13039/501100011033 and by ERDF, UE. VR also acknowledges support from the grant number RYC2020-029387-I funded by MICIU/AEI/10.13039/501100011033 and by “ESF, Investing in your future,” and from the Consejo Superior de Investigaciones Científicas (CSIC) and the Centro de Astrobiología (CAB) through the project 20225AT015 (Proyectos intramurales especiales del CSIC). IJ-S also acknowledges support by ERC grant OPENS, GA No. 101125858, funded by the European Union. M.S.-N. IJ-S. acknowledge funding from Consejo Superior de Investigaciones Científicas (CSIC) through project i-LINK23017 SENTINEL. MS-N also acknowledges a Juan de la Cierva Postdoctoral Fellowship, project JDC2022-048934-I, funded

by MCIN/AEI/10.13039/501100011033 and by the European Union “NextGenerationEU/PRTR.”

## Acknowledgements

Mitsunori Araki is acknowledged for useful insights regarding the theoretical calculations.

## Conflict of interest

The authors declare that the research was conducted in the absence of any commercial or financial relationships that could be construed as a potential conflict of interest.

## Generative AI statement

The authors declare that no Generative AI was used in the creation of this manuscript.

Any alternative text (alt text) provided alongside figures in this article has been generated by Frontiers with the support of artificial intelligence and reasonable efforts have been made to ensure accuracy, including review by the authors wherever possible. If you identify any issues, please contact us.

## Publisher's note

All claims expressed in this article are solely those of the authors and do not necessarily represent those of their affiliated organizations, or those of the publisher, the editors and the reviewers. Any product that may be evaluated in this article, or claim that may be made by its manufacturer, is not guaranteed or endorsed by the publisher.

## Author disclaimer

Views and opinions expressed are however those of the author(s) only and do not necessarily reflect those of the European Union or the European Research Council Executive Agency. Neither the European Union nor the granting authority can be held responsible for them.

## Supplementary material

The Supplementary Material for this article can be found online at: <https://www.frontiersin.org/articles/10.3389/fchem.2025.1720662/full#supplementary-material>

## References

- April, R. (1986). Sulfur, its significance for chemistry, for the Geo-Bio- and cosmospere and technology. *Earth Sci. Rev.* 23, 229–230. doi:10.1016/0012-8252(86)90023-1
- Araki, M., Lattanzi, V., Endres, C. P., and Caselli, P. (2024). Millimeter and submillimeter spectroscopy of the deuterated molecular ion SD<sup>+</sup>. *Astrophysical J.* 965, 46. doi:10.3847/1538-4357/ad2f9d

- Asplund, M., Grevesse, N., Sauval, A. J., and Scott, P. (2009). The chemical composition of the sun. *Annu. Rev. Astron. Astrophys.* 47, 481–522. doi:10.1146/annurev.astro.46.060407.145222
- Barone, V., Uribe, L., Srivastav, S., and Pathak, A. (2024). Toward accurate characterization of the puzzling NSO and SNO moieties. *ACS Earth Space Chem.* 8, 2334–2344. doi:10.1021/acsearthspacechem.4c00256
- Bizzocchi, L., Lattanzi, V., Laas, J., Spezzano, S., Giuliano, B. M., Prudeniano, D., et al. (2017). Accurate sub-millimetre rest frequencies for HOCO<sup>+</sup> and DOCO<sup>+</sup> ions. *Astronomy Astrophysics* 602, A34. doi:10.1051/0004-6361/201730638
- Chang, Y., Fu, Y., Chen, Z., Luo, Z., Zhao, Y., Li, Z., et al. (2023). Vacuum ultraviolet photodissociation of sulfur dioxide and its implications for oxygen production in the early earth's atmosphere. *Chem. Sci.* 14, 8255–8261. doi:10.1039/D3SC03328G
- Dal Borgo, A., Hermanns, M., and Winnewisser, M. (1979). CIDNP transfer nuclear dipolar relaxation and spin-spin coupling. *Chem. Phys. Lett.* 62, 421–426. doi:10.1016/0009-2614(79)80733-2
- Dore, L. (2003). Using fast fourier transform to compute the line shape of frequency-modulated spectral profiles. *J. Mol. Spectrosc.* 221, 93–98. doi:10.1016/S0022-2852(03)00203-0
- Dunning, T. H., Peterson, K. A., and Wilson, A. K. (2001). Gaussian basis sets for use in correlated molecular calculations. x. The atoms aluminum through argon revisited. *J. Chem. Phys.* 114, 9244–9253. doi:10.1063/1.1367373
- Filipovic, M. R., Miljkovic, J. L., Nauser, T., Royzen, M., Klos, K., Shubina, T., et al. (2012). Chemical characterization of the smallest s-nitrosothiol, hns; cellular cross-talk of h2s and s-nitrosothiols. *JACS* 134, 12016–12027. doi:10.1021/ja3009693
- García de la Concepción, J., Jiménez-Serra, I., Carlos Corchado, J., Rivilla, V. M., and Martín-Pintado, J. (2021). The origin of the E/Z isomer ratio of imines in the interstellar medium. *Astrophysical J. Lett.* 912, L6. doi:10.3847/2041-8213/abf650
- García de la Concepción, J., Colzi, L., Jiménez-Serra, I., Molpeceres, G., Corchado, J. C., Rivilla, V. M., et al. (2022). The trans/cis ratio of formic (hcooh) and thioformic (hc(oh)sh) acids in the interstellar medium. *Astronomy Astrophysics* 658, A150. doi:10.1051/0004-6361/202142287
- Gómez Martín, J. C., Brooke, J. S. A., Feng, W., Höpfner, M., Mills, M. J., and Plane, J. M. C. (2017). Impacts of meteoric sulfur in the earth's atmosphere. *J. Geophys. Res. Atmos.* 122, 7678–7701. doi:10.1002/2017jd027218
- Heineking, N., and Gerry, M. C. L. (1993). Hyperfine structures in the rotational spectra of thionylimide (hns) and thionylimide-d<sub>1</sub> (dnso). *J. Mol. Spectrosc.* 160, 164–176. doi:10.1006/jmsp.1993.1187
- Herath, A., McAnally, M., Turner, A. M., Wang, J., Marks, J. H., Fortenberry, R. C., et al. (2025). Missing interstellar sulfur in inventories of polysulfanes and molecular octasulfur crowns. *Nat. Commun.* 16, 5571. doi:10.1038/s41467-025-61259-2
- Inostroza-Pino, N., Lattanzi, V., Palmer, C. Z., Fortenberry, R. C., Mardones, D., Caselli, P., et al. (2024). Rotational spectroscopic characterisation of the [d<sub>2</sub>c<sub>s</sub>] system: an update from the laboratory and theory. *Mol. Phys.* 122, e2280762. doi:10.1080/00268976.2023.2280762
- Ivanova, L. V., Anton, B. J., and Timerghazin, Q. K. (2014). On the possible biological relevance of hns isomers: a computational investigation. *Phys. Chem. Chem. Phys.* 16, 8476–8486. doi:10.1039/C4CP00469H
- Jiang, X., Fan, Y., Huang, L., Guo, Y., Fang, W., Wang, L., et al. (2025). Deciphering the photochemistry of thionylimide (hns): isomers and tunneling-controlled reactions. *J. Am. Chem. Soc.* 147, 28173–28178. doi:10.1021/jacs.5c08291
- Jiménez-Serra, I., Rodríguez-Almeida, L. F., Rivilla, V. M., Melosso, M., and Zeng, S. (2022). Precursors of fatty alcohols in the ism: discovery of n-propanol. *Astronomy Astrophysics* 663, A181. doi:10.1051/0004-6361/202142699
- Kirchhoff, W. H., Johnson, D. R., and Duncan, A. B. (1969). Microwave spectrum and dipole moment of cis-thionylimide (hns). *J. Am. Chem. Soc.* 91, 1113–1117. doi:10.1021/ja01030a012
- Krasnopolsky, V. A. (2012). A photochemical model for the venus atmosphere at 47–112km. *Icarus* 218, 230–246. doi:10.1016/j.icarus.2011.11.012
- Kumar, M., and Francisco, J. S. (2017). Energetics and interconversion pathways of hns and related isomers. *J. Phys. Chem. A* 121, 1127–1136. doi:10.1021/acs.jpca.6b12031
- Laas, J. C., and Caselli, P. (2019). Modeling sulfur depletion in interstellar clouds. *Astronomy Astrophysics* 624, A108. doi:10.1051/0004-6361/201834446
- Lattanzi, V., Thaddeus, P., McCarthy, M. C., and Thorwirth, S. (2010). Laboratory detection of protonated SO<sub>2</sub> in two isomeric forms. *J. Chem. Phys.* 133, 194305. doi:10.1063/1.3491510
- Lattanzi, V., Spezzano, S., Laas, J. C., Chantzos, J., Bizzocchi, L., Lee, K. L. K., et al. (2018). HSCO<sup>+</sup> and DSCO<sup>+</sup>: a multi-technique approach in the laboratory for the spectroscopy of interstellar ions. *Astronomy Astrophysics* 620, A184. doi:10.1051/0004-6361/201834340
- Lattanzi, V., Sanz-Novo, M., Rivilla, V. M., Araki, M., Bunn, H. A., Martín-Pintado, J., et al. (2024). Advancing spectroscopic understanding of HOCs<sup>+</sup>: laboratory investigations and astronomical implications. *Astronomy Astrophysics* 689, A260. doi:10.1051/0004-6361/202451518
- Lattalais, M., Pauzat, F., Ellinger, Y., and Ceccarelli, C. (2009). Interstellar complex organic molecules and the minimum energy principle. *Astrophysical J. Lett.* 696, L133–L136. doi:10.1088/0004-637x/696/2/l133
- Martín, S., Martín-Pintado, J., Blanco-Sánchez, C., Rivilla, V. M., Rodríguez-Franco, A., and Rico-Villas, F. (2019). Spectral line identification and modelling (SLIM) in the MADrid data CUBe analysis (MADCUBA) package. Interactive software for data cube analysis. *Astrophysical J.* 631, A159. doi:10.1051/0004-6361/201936144
- Matthews, D. A., Cheng, L., Harding, M. E., Lipparini, F., Stopkowicz, S., Jagau, T.-C., et al. (2020). Coupled-cluster techniques for computational chemistry: the CFOUR program package. *J. Chem. Phys.* 152, 214108. doi:10.1063/5.0004837
- Miljkovic, J. L., Kenkel, I., Ivanović-Burmazović, I., and Filipovic, M. R. (2013). Generation of hno and hns from nitrite by heme-iron-catalyzed metabolism with h<sub>2</sub>s. *Angew. Chem. Int. Ed.* 52, 12061–12064. doi:10.1002/anie.201305669
- Mininni, C., Beltrán, M. T., Rivilla, V. M., Sánchez-Monge, A., Fontani, F., Möller, T., et al. (2020). The GUAPOS project: G31.41+0.31 unbiased ALMA sPectral observational survey. I. Isomers of C<sub>2</sub>H<sub>4</sub>O<sub>2</sub>. *Astronomy Astrophysics* 644, A84. doi:10.1051/0004-6361/202038966
- Molpeceres, G., Agúndez, M., Mallo, M., Cabezas, C., Sanz-Novo, M., Rivilla, V. M., et al. (2025). Piecing together formic acid isomerism in dark clouds. Detection of cis-formic acid in TMC-1 and astrochemical modeling.
- Perdigón, J., de Laverny, P., Recio-Blanco, A., Fernandez-Alvar, E., Santos-Peral, P., Kordopatis, G., et al. (2021). The AMBRE project: origin and evolution of sulfur in the Milky Way. *Astronomy Astrophysics* 647, A162. doi:10.1051/0004-6361/202040147
- Peterson, K. A., and Dunning, T. H. (2002). Accurate correlation consistent basis sets for molecular core-valence correlation effects: the second row atoms Al–Ar, and the first row atoms B–Ne revisited. *J. Chem. Phys.* 117, 10548–10560. doi:10.1063/1.1520138
- Prudeniano, D., Laas, J., Bizzocchi, L., Lattanzi, V., Endres, C., Giuliano, B. M., et al. (2018). Accurate millimetre and submillimetre rest frequencies for cis- and trans-thioformic acid, HCSSH. *Astronomy Astrophysics* 612, A56. doi:10.1051/0004-6361/201732397
- Puskar, L., Robertson, E. G., and McNaughton, D. (2006). High-resolution FTIR spectroscopy of HNSO—Analysis of the highly perturbed ν<sub>4</sub>, ν<sub>6</sub> and 2 ν<sub>5</sub> bands. *J. Mol. Spectrosc.* 240, 244–250. doi:10.1016/j.jms.2006.10.001
- Raghavachari, K., Trucks, G. W., Pople, J. A., and Head-Gordon, M. (1989). A fifth-order perturbation comparison of electron correlation theories. *Chem. Phys. Lett.* 157, 479–483. doi:10.1016/S0009-2614(89)87395-6
- Requena-Torres, M. A., Martín-Pintado, J., Martín, S., and Morris, M. R. (2008). The galactic center: the largest oxygen-bearing organic molecule repository. *Astrophysical J.* 672, 352–360. doi:10.1086/523627
- Richardson, C. D., Hinman, N. W., and Scott, J. R. (2013). Evidence for biological activity in mineralization of secondary sulphate deposits in a basaltic environment: implications for the search for life in the Martian subsurface. *Int. J. Astrobiol.* 12, 357–368. doi:10.1017/S1473550413000256
- Rivilla, V. M., Martín-Pintado, J., Jiménez-Serra, I., Zeng, S., Martín, S., Armijos-Abendaño, J., et al. (2019). Abundant Z-cyanomethanimine in the interstellar medium: paving the way to the synthesis of adenine. *Mon. Notices R. Astronomical Soc.* 483, L114–L119. doi:10.1093/mnras/sly228
- Rivilla, V. M., Sanz-Novo, M., Jiménez-Serra, I., Martín-Pintado, J., Colzi, L., Zeng, S., et al. (2023). First glycine isomer detected in the interstellar medium: Glycolamide (NH<sub>2</sub>C(O)CH<sub>2</sub>OH). *Astrophysical J. Lett.* 953, L20. doi:10.3847/2041-8213/ace977
- San Andrés, D., Rivilla, V. M., Colzi, L., Jiménez-Serra, I., Martín-Pintado, J., Megías, A., et al. (2024). First detection in space of the high-energy isomer of cyanomethanimine: H<sub>2</sub>CNCN. *Astrophysical J.* 967, 39. doi:10.3847/1538-4357/ad3af3
- Sanz-Novo, M., Rivilla, V. M., Jiménez-Serra, I., Martín-Pintado, J., Colzi, L., Zeng, S., et al. (2023). Discovery of the elusive carbonic acid (HOCOOH) in space. *Astrophysical J.* 954, 3. doi:10.3847/1538-4357/ace523
- Sanz-Novo, M., Rivilla, V. M., Jiménez-Serra, I., Martín-Pintado, J., Colzi, L., Zeng, S., et al. (2024). Interstellar detection of O-protonated carbonyl sulfide, HOCs<sup>+</sup>. *Astrophysical J.* 965, 149. doi:10.3847/1538-4357/ad2c01
- Sanz-Novo, M., Rivilla, V. M., Müller, H. S. P., Jiménez-Serra, I., Martín-Pintado, J., Colzi, L., et al. (2024). Discovery of thionylimide, hns, in space: the first n-s- and o-bearing interstellar molecule. *Astrophysical J. Lett.* 965, L26. doi:10.3847/2041-8213/ad3945
- Shingledecker, C. N., Álvarez-Barcia, S., Korn, V. H., and Kästner, J. (2019). The case of H<sub>2</sub>C<sub>3</sub>O isomers, revisited: solving the mystery of the missing propadienone. *Astrophysical J.* 878, 80. doi:10.3847/1538-4357/ab1d4a
- Shingledecker, C. N., Lamberts, T., Laas, J. C., Vasyunin, A., Herbst, E., Kästner, J., et al. (2020). Efficient production of S<sub>8</sub> in interstellar ices: the effects of cosmic-ray-driven radiation chemistry and nondiffusive bulk reactions. *Astrophysical J.* 888, 52. doi:10.3847/1538-4357/ab5360
- Todd, Z. R. (2022). Sources of nitrogen-sulfur-and phosphorus-containing feedstocks for prebiotic chemistry in the planetary environment. *Life* 12, 1268. doi:10.3390/life12081268

Wheeler, S. E., Yamaguchi, Y., and Schaefer, H. F. (2006). Protonated carbonyl sulfide: prospects for the spectroscopic observation of the elusive  $\text{HSCO}^+$  isomer. *J. Chem. Phys.* 124, 044322. doi:10.1063/1.2150819

Wu, D., Hu, Q., and Zhu, D. (2018). An update on hydrogen sulfide and nitric oxide interactions in the cardiovascular system. *Oxidative Med. Cell. Longev.* 2018, 4579140. doi:10.1155/2018/4579140

Yang, X. J., Hua, L., and Li, A. (2024). Where have all the sulfur atoms gone? Polycyclic aromatic hydrocarbon as a possible sink for the missing sulfur in the interstellar medium. I. The C–S band strengths. *Astrophysical J.* 974, 30. doi:10.3847/1538-4357/ad6dd7

Zeng, S., Jiménez-Serra, I., Rivilla, V. M., Martín, S., Martín-Pintado, J., Requena-Torres, M. A., et al. (2018). Complex organic molecules in the galactic centre: the N-bearing family. *Mon. Notices R. Astronomical Soc.* 478, 2962–2975. doi:10.1093/mnras/sty1174

Zeng, S., Rivilla, V. M., Sanz-Novo, M., Melosso, M., Jiménez-Serra, I., Colzi, L., et al. (2025). High-energy interstellar isomers: cis-n-methylformamide in the G+0.693-0.027 molecular cloud. *Astron. Astrophys.* 703, A73. doi:10.1051/0004-6361/202556709

Zhao, Y., Wang, Y., Xu, Q., Zhou, K., Shen, Y., Guo, L., et al. (2024). Hydrogen sulfide donors across time: from origins to cutting-edge applications. *Nitric Oxide* 144, 29–39. doi:10.1016/j.niox.2024.01.003